

Biofriendly, Stretchable, and Reusable Hydrogel Electronics as Wearable Force Sensors

Hao Liu, Moxiao Li, Cheng Ouyang, Tian Jian Lu, Fei Li,* and Feng Xu*

The ever-growing overlap between stretchable electronic devices and wearable healthcare applications is igniting the discovery of novel biocompatible and skin-like materials for human-friendly stretchable electronics fabrication. Amongst all potential candidates, hydrogels with excellent biocompatibility and mechanical features close to human tissues are constituting a promising troop for realizing healthcare-oriented electronic functionalities. In this work, based on biocompatible and stretchable hydrogels, a simple paradigm to prototype stretchable electronics with an embedded three-dimensional (3D) helical conductive layout is proposed. Thanks to the 3D helical structure, the hydrogel electronics present satisfactory mechanical and electrical robustness under stretch. In addition, reusability of stretchable electronics is realized with the proposed scenario benefiting from the swelling property of hydrogel. Although losing water would induce structure shrinkage of the hydrogel network and further undermine the function of hydrogel in various applications, the worn-out hydrogel electronics can be reused by simply casting it in water. Through such a rehydration procedure, the dehydrated hydrogel can absorb water from the surrounding and then the hydrogel electronics can achieve resilience in mechanical stretchability and electronic functionality. Also, the ability to reflect pressure and strain changes has revealed the hydrogel electronics to be promising for advanced wearable sensing applications.

and deformability of electronic devices are crucial to achieving their functionalities. Meanwhile, as the interface bridging human tissues and electronic functionalities, the substrate material for stretchable electronics needs to be highly biocompatible to realize long-time integration with delicate human tissues for healthcare monitoring. This unprecedented demand has called for the employment of soft biomaterials in stretchable electronics fabrication.

Hydrogel is well known to be a bio-origin soft material. The extensive uses of hydrogel in tissue engineering^[12–14] and drug delivery^[15,16] have clearly outlined its incomparable biocompatibility and favorable human tissue-like mechanical property. Besides, hydrogel is of excellent molecular permeability and can be modified with functional biomolecules, further improving the integration of hydrogel and human physiological environment.^[17] These appealing features pledge hydrogel to outperform other soft materials (e.g., silicon elastomer^[18,19]) in fabricating stretchable electronics, especially those targeting at human-


friendly wearable or implantable applications. However, the currently available scenarios for fabricating hydrogel-based stretchable electronics^[20–22] are associated with some intrinsic warts, which may induce potential obstruction to its practical application. One obstacle lies in the selection of conductive fillers. Specifically, conductive elements like sodium chloride^[20,21] and titanium^[22] are associated with relatively low

1. Introduction

Soft and stretchable electronics has been igniting marvelous research sparks during the past decade, especially with rapidly increasing interests for biorelated applications, such as implantable physiological monitoring^[1–4] and wearable healthcare tracking.^[5–11] For these applications, the softness

H. Liu, C. Ouyang, Dr. F. Li, Prof. F. Xu
The Key Laboratory of Biomedical Information Engineering
of Ministry of Education
School of Life Science and Technology
Xi'an Jiaotong University
Xi'an 710049, P. R. China
E-mail: feili@mail.xjtu.edu.cn; fengxu@mail.xjtu.edu.cn

H. Liu, M. Li, C. Ouyang, Prof. T. J. Lu, Dr. F. Li, Prof. F. Xu
Bioinspired Engineering and Biomechanics Center (BEBC)
Xi'an Jiaotong University
Xi'an 710049, P. R. China

 The ORCID identification number(s) for the author(s) of this article can be found under <https://doi.org/10.1002/sml.201801711>.

M. Li
State Key Laboratory for Strength and Vibration of
Mechanical Structures
Aerospace School
Xi'an Jiaotong University
Xi'an 710049, P. R. China
Prof. T. J. Lu
MOE Key Laboratory for Multifunctional Materials and Structures
Xi'an Jiaotong University
Xi'an 710049, P. R. China
Prof. T. J. Lu
College of Aerospace Engineering
Nanjing University of Aeronautics and Astronautics
Nanjing 210016, P. R. China

DOI: 10.1002/sml.201801711

conductivity, hence causing unnecessarily large power consumption. Besides, compulsory oxygen plasma treatment and silane functionalization procedures further complicate the as-reported fabrication process for hydrogel-based electronics,^[22] which inevitably raises the fabrication cost and sets back its widespread applications, especially those catering to impoverished users in rural regions. In addition, in spite of the use of tough hydrogels as substrate, the 2D serpentine layout of conductive elements may constrain the mechanical stretchability and robustness of hydrogel electronics as a whole due to the potential fracture resulting from stress concentrations occurring to such 2D structure.^[22] Besides, the delamination of solid titanium wires from the elastomeric hydrogel substrate may also occur under large strains, which can be circumvented by embedding conductive liquids into the soft substrate.^[23]

Additional attention should be paid that owing to its swelling property, even a piece of dehydrated hydrogel with shrunken and rigid body can absorb water from the ambience to recover to its original size and softness through hydration.^[24,25] In this way, hydrogel-based products hold great potential to be reusable. For example, it is possible for worn-out hydrogel-based electronic devices which fail to work in the right way because of hydrogel dehydration to be reused by simply rehydrating in water to bring the mechanical deformability and electronic functionality back to life. To note that, this reusable capability is of considerable importance to coping with the recycling/disposal issue and practical difficulties in device collection/reprocessing of electronic products, especially considering the massive electronic wastes made worldwide. Further, reusing electronics reduces the number of electronic items that need to be made and thus benefits conserving natural resources and raw materials required for electronics manufacturing. In addition, once commercialized, reusable electronics with well sustained functionality are anticipated to help consumers to save relevant expenditure compared to buying single-use electronics items. However, to the best of our knowledge, the reusability of stretchable electronics has been barely investigated. Therefore, it is still an unresolved challenge to fabricate stretchable hydrogel electronics with highly conductive filler elements, easily accessible fabrication, robust conductive element layout as well as reusable ability closely related to practical applications.

Herein, we proposed a facile microfluidic paradigm to prototype stretchable electronics based on biocompatible and stretchable hydrogels, and used polyacrylamide (PAA)-alginate hydrogel as a demonstration. Super conductive liquid metal (EGaIn, resistivity of $\approx 29.4 \times 10^{-6} \Omega \text{ cm}$),^[18,26,27] a room temperature liquid-phase eutectic, was employed to serve as the conductive element filling 3D microfluidic channels embedded in the hydrogel matrix. The hydrogel electronics presents satisfactory electrical robustness under mechanical stretch ($\approx 10\%$ resistance change for up to 300 cycles) thanks to the 3D helical-shaped conductive network. In addition, the prepared hydrogel electronics has been proved reusable since the disabled hydrogel electronics as a result of hydrogel dehydration could experience rebirth with acceptable property and functional resilience. Furthermore, the as-fabricated hydrogel electronics has been demonstrated to be feasible as a

body-worn motion detector, representing colossal potential for the cutting-edge human-friendly wearable uses.

2. Results and Discussions

2.1. Fabrication of the Hydrogel Electronics

The microfluidic fabrication process of the hydrogel electronics started with injecting PAA-alginate precursor solution into a poly(methyl methacrylate) (PMMA) casting mold, which was inserted with a helical spring from one side of the chamber (Figure 1). The PMMA chamber filled with PAA-alginate precursor was then successively transferred into an oven at 70 °C for 3 h (covalent crosslinking of PAA) and immersed into 0.1 M CaCl₂ solution for another 3 h (ionic crosslinking of alginate) to produce PAA-alginate hydrogel. To note that, PAA-alginate is a double network hydrogel where PAA network and alginate network interpenetrate with each other. The PAA network is achieved by heating, while the divalent Ca²⁺ ions in the CaCl₂ aqueous solution are responsible for forming ionic crosslinks among alginate monomers to obtain alginate hydrogel. Subsequently, the preinserted helical spring was rotated out of the hydrogel and a transparent 3D microfluidic channel was formed inside the hydrogel. In the following step, liquid metal was injected into the helical microchannel and copper wires were connected to both ends of the channel to facilitate interconnection of the hydrogel electronics with outer circuits. Next, the hydrogel electronics was finally realized via sealing with a thin layer of PAA on both sides of the hydrogel to avoid leaking of liquid metal under mechanical stretch.

Benefiting from its fluid nature at room temperature, the liquid metal can readily flow to conform the intense deformation of the embedded helical channel when the hydrogel substrate is stretched (Figure 2a). This intriguing feature helps to eliminate disconnection of stretchable electronics that is often associated with the fracture of solid-state conductive fillers, especially at high strain levels. Also, liquid metal is of high surface tension and density, making it impermeable to hydrogel matrix.^[26] This unique property helps liquid metal to outperform other possible liquid-phase conductive fillers (e.g., ionic electrolyte, graphene oxide nanoparticles) which are usually aqueous solutions and may unexpectedly diffuse into hydrogel matrix. The finite element simulation result of strain distribution agrees well with that of the experiment, as reflected by digital photos of the hydrogel electronics under different strain levels. In principle, stress presents uniform distribution in helical structure inside hydrogel matrix without localized concentrations even at large levels of strain (e.g., 300%) (Figure 2a; Figure S1, Supporting Information). This result ascribed from the 3D helical layout is beneficial to enhance the mechanical stretchability and robustness of hydrogel electronics. The fabricated hydrogel electronics is also capable of strain sensing, as elucidated by its obvious resistance change as a function of strain (Figure 2b). For instance, resistance of the hydrogel electronics at 300% strain rises up to twice as much as that in the unstretched state (R_0). The underlying mechanism behind the strain sensing ability lies in the deformation

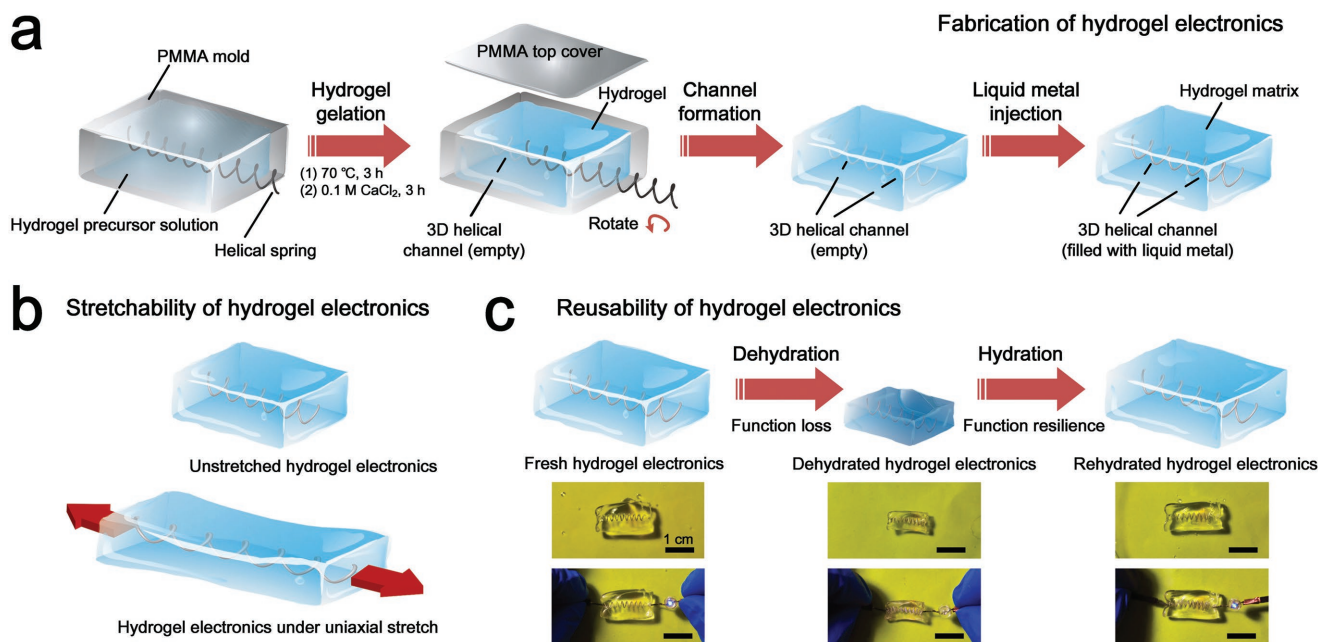


Figure 1. Schematic illustration of the hydrogel electronics. a) Detailed fabrication process of the hydrogel electronics. b) Schematic demonstration of the stretchability of the hydrogel electronics. c) Schematics (top) and digital photos (middle and bottom) to demonstrate the change in size and electrical conductivity of the hydrogel electronics during dehydration/hydration process. This phenomenon unlocks the feasibility of hydrogel electronics for reusable applications (i.e., hydrogel electronics with function-failure due to hydrogel hydration can realize functional resilience via rehydration).

of the liquid metal-filled embedded channel when hydrogel is stretched. Since the elongation of the 3D helical channel is minimal and negligible until it is stretched to fully straight, the resistance change of the hydrogel electronics mainly depends on the variance of the cross-sectional area of the channel under deformation. The corresponding resistance (R) of the hydrogel electronics at different strain levels can be calculated as Equation (1)

$$R = \rho \int \frac{1}{s} dl \quad (1)$$

where ρ is the electrical resistivity of liquid metal, l is the equivalent length of the 3D helical channel, and s is the cross-sectional area of the channel. When the hydrogel matrix is under the same level of uniaxial strain, the total deformation of embedded 3D helical structure is remarkably lower compared to those of traditionally used conductive layouts (namely 1D line and 2D serpentine) for soft electronics fabrication. The 1D line structure elongates along with the stretch direction, as well as shrinks in cross-section area due to Poisson ratio, making it sensitive but vulnerable to mechanical stretch. The 2D serpentine construct fails to uniformly distribute stress ascribed from hydrogel deformation, so it is often associated with stress concentrations which may cause potential fracture of the conductive network under large levels of strain.^[28] This is supported by the experimental result that hydrogel electronics with 1D line or 2D serpentine layout fails to function under large deformation with observable liquid metal disconnection (150% strain for 1D line structure and 250% strain for 2D serpentine structure) as a result of stretch-caused channel deformation (Figure S2, Supporting Information). So the 3D helical format which enables response to as

large as 300% strain turns out to be an optimal selection for fabricating hydrogel electronics with enhanced stretchability and robustness. And by employing helical springs with different pitch gauge values (i.e., helical densities) which brings about varying s change of embedded channel when the hydrogel is stretched, the strain sensing curve of the hydrogel electronics can be flexibly adjusted to cater for demands of different working circumstances (Figure S3, Supporting Information). In addition, a fatigue test was carried out to test the electrical stability of the hydrogel conductor against cyclic stretch. The testing result indicates that only $\approx 10\%$ change in resistance occurs after 300 repeating cycles of stretch-release (Figure 2c).

2.2. Reusability of the Hydrogel Electronics

Considering the increasingly large number of global electronic wastes produced in the contemporary world and ecological concerns on valuable natural resources and energies consumed in electronics manufacturing, electronic devices that can be reused and perform as original even after function failure may offer a promising way out of these issues. Such reusable electronics with well recovered functionality are highly favored to replace their single-use counterparts. Based on the swelling capacity of hydrogel, we tested the feasibility of the proposed hydrogel electronics for reusable applications. To mimic its function failure caused by hydrogel dehydration, we dried the hydrogel electronics in a heating oven at 70 °C for 3 h. It can be observed that, compared to that in initial state, the hydrogel electronics shrinks in size and loses its function since it cannot light up a light emitting

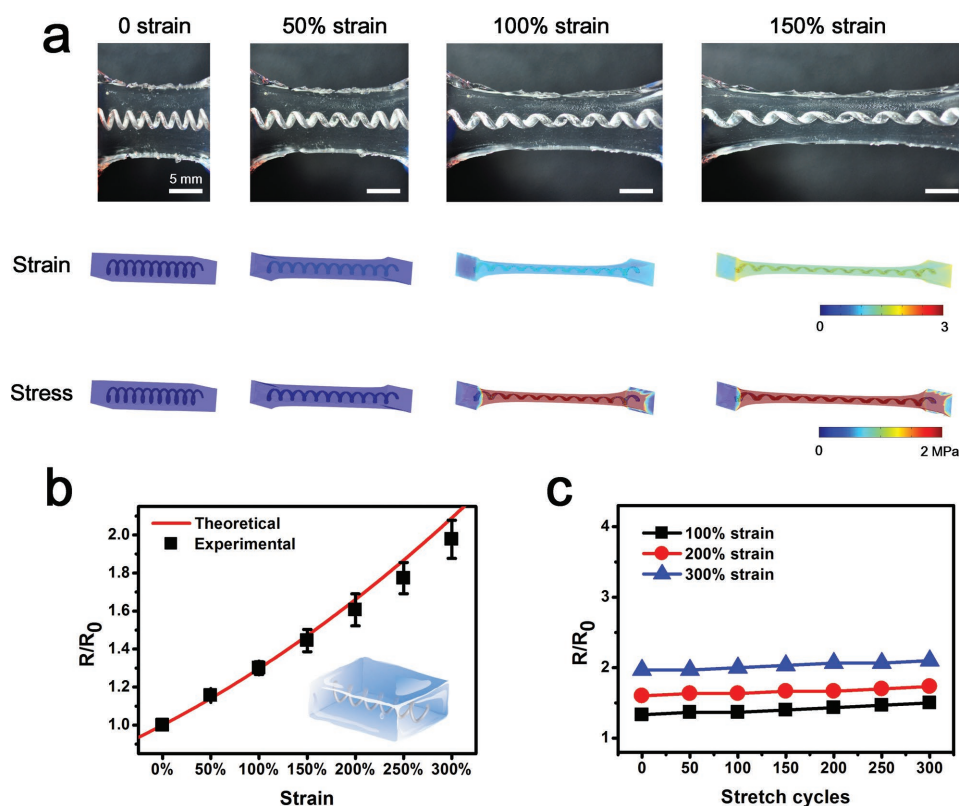


Figure 2. Performance of the hydrogel electronics under cyclic mechanical stretch. a) Digital photos and FEA simulation results (strain and stress distribution) of hydrogel electronics under different levels of strain. Electrical characterization of the hydrogel electronics: b) resistance versus different strain levels and c) resistance versus different stretch cycles. Error bars represent standard deviation ($N = 3$).

diode (LED) after being dried (Figure 3a). However, when we soaked the dehydrated hydrogel electronics in water for another 3 h, it recovers to its original size and the connected LED glows again to demonstrate the functional resilience. In other words, the dehydrated hydrogel electronics can be reused. Such interesting phenomenon is closely associated with the swelling mechanism of hydrogel. More specifically, hydrogel is well known to be a 3D cross-linked polymerized system with water content of more than 90%, so it is understandable that hydrogel decreases in size and loses weight along with the moisture loss in drying process. Also, losing moisture will shrink the polymer network of hydrogel. To note that, the shrinkage is nonuniform as observed, so large degrees of contraction may occur in some specific sites inside the hydrogel to block the continuous flow of embedded liquid metal, resulting in disconnection and going off of the LED. When put into water, the hydrogel electronics can adsorb water, swell, and recover in size, weight, and further electrical conductivity. Experimental results show that after 70 °C heat-drying for 3 h, the hydrogel electronics loses $\approx 80\%$ of its initial weight, and an extra 3 h soaking in water can well bring it back ($>85\%$ of its initial weight) even after 30 drying–soaking cycles (Figure 3b; Figure S4a, Supporting Information). By simply soaking in water with longer time, the dehydrated hydrogel electronics can perform higher levels of resilience in mass ($\sim 100\%$ of its initial weight) (Figure S4b, Supporting Information). Relevant tensile tests were also implemented to study the stretchability resilience of the hydrogel

electronics (Figure 3c; Figure S5, Supporting Information). Although Young's modulus of hydrogel electronics experiences an observable rise along with increasing drying–soaking cycle number due to the water absorbed in swelling process which lowers the concentration of polymer, it is still suitable for wearable uses considering the well matching with the mechanical property of human skin (Young's modulus of $1\text{--}10^5$ kPa^[29]). Furthermore, the hydrogel electronics exhibits $\approx 30\%$ relative increase in resistance, possibly as a result of the decreasing cross-sectional area of the embedded liquid metal when the hydrogel matrix swells inward to compress the channel (Figure 3d). And its strain sensing ability functions steadily even after numerous repeating cycles of drying and soaking (Figure 3e). Thus, it can be concluded that such hydrogel electronics can be reused with acceptable level of functionality recovery even after severe dehydration, and the reusable capability shows decent cyclic performance (for as many as 30 drying–soaking cycles).

To further investigate the reusable performance (i.e., functional failure-resilience performance) of the hydrogel electronics, experimental parameters in dehydration and rehydration process need to be carefully optimized. Proper material selection for sealing is of great importance to avoid leakage of liquid metal from helical channels embedded in the hydrogel matrix when the hydrogel electronics is under mechanical stretch for practical using or during drying process to mimic function failure. So we tested the electrical conductivity change of the hydrogel electronics during drying process using three

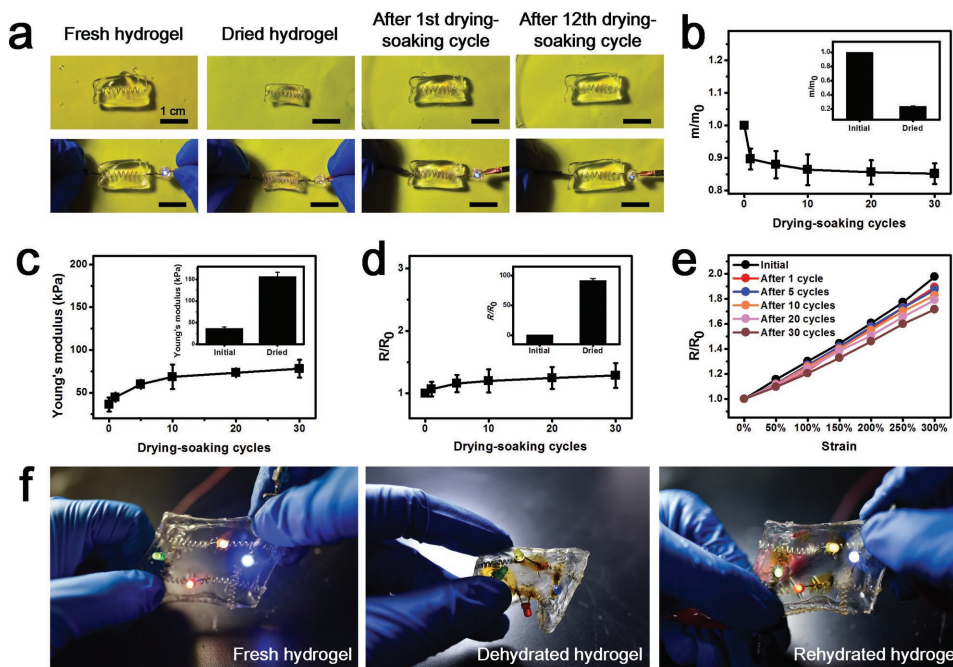


Figure 3. Reusability of the hydrogel electronics. a) Digital photos of hydrogel electronics in different conditions: initial, dried, after enduring the 1st drying–soaking cycle and after enduring the 12th drying–soaking cycle. b) Mass, c) Young’s modulus, and d) electrical resistance changes of the hydrogel electronics as a function of drying–soaking cycle numbers. Insets are corresponding property comparison of fresh hydrogel electronics and dried hydrogel electronics. Error bars represent standard deviation ($N = 3$). e) Strain sensing curves of the hydrogel electronics after enduring different numbers of drying–soaking cycle. f) Reusability demonstration of a LED display based on hydrogel electronics. The stable performance of the LED display under stretch (left). The hydrogel becomes rigid and cannot be stretched when dehydrated (or dried) and the function of the LED display is thus “locked” (middle). The functional resilience (mechanical stretchability and electrical functionality) of the hydrogel-based LED display after rehydration in water environment (right).

different sealing material candidates, i.e., polydimethylsiloxane (PDMS), polyethylene glycol (PEG) and PAA. We clearly observed that compared to the unsealed group and those sealed with PDMS or PEG, hydrogel electronics sealed with PAA can survive longer drying period (3 h) with maintained electrical conductivity, making it a prior choice for sealing hydrogel electronics (Figure S6a, Supporting Information). Other candidate sealing materials may include cyanoacrylate-based adhesives which can diffuse into hydrogel matrix, and further realize mechanically tough bonding of hydrogels via interlayer tough bonds.^[30] It has been proved that the bonded hydrogel can survive intense deformation without fracture or functionality failure. So it is promising to utilize such adhesive for sealing the microchannels inside hydrogel matrix in a tough manner, in case of liquid metal leakage under stretch or dehydration of hydrogel. Apart from the sealing material selection, the time for drying also plays a vital part in promoting resilience performance of the hydrogel electronics. Longer period of drying time induces dramatic loss and poor recovery of electrical property of the hydrogel electronics during the whole drying–soaking process (Figure S6a,b, Supporting Information). One possible reason may be that the polymer network inside hydrogel shrinks intensely in long-time drying and then squeezes the conductive filler (i.e., liquid metal) out of the hydrogel (blue dotted circles in the enlarged photos of Figure S6c in the Supporting Information). Meanwhile, drying time and soaking time also determine the resilience of mechanical

stretchability of the hydrogel electronics (Figure S7, Supporting Information).

In addition, an LED display based on hydrogel electronics was employed to further testify the practical significance of reusing issue (Figure 3f; Movie S1, Supporting Information). The LEDs were mounted on a piece of hydrogel with cross-connected helical conductive traces and the whole display device was then wired to a power supply to establish the test circuit (Figure S8, Supporting Information). The hydrogel-based LED display performed robustly even under intense stretch (Figure 3f, left). While after being dehydrated, the hydrogel became rigid due to the loss of moisture and thus could not be stretched (Figure 3f, middle). Further, since the LEDs found no shine on the dehydrated hydrogel and the total mass of the device experienced $\approx 80\%$ loss (from 11.73 to 2.07 g) in dehydration, it could be concluded that the function of the hydrogel-based LED display was “locked” in light weight. Luckily, a simple rehydration procedure in which the dehydrated device was soaked into water for 3 h could bring about the resilience of mechanical stretchability as well as electrical functionality of the hydrogel-based LED display (Figure 3f, right). Despite that local color change can be observed on the hydrogel due to the rust of LED pins after long-time integration, it can be mitigated through coating a thin layer of PDMS on the pin to block moisture from the hydrogel (Figure S9, Supporting Information).

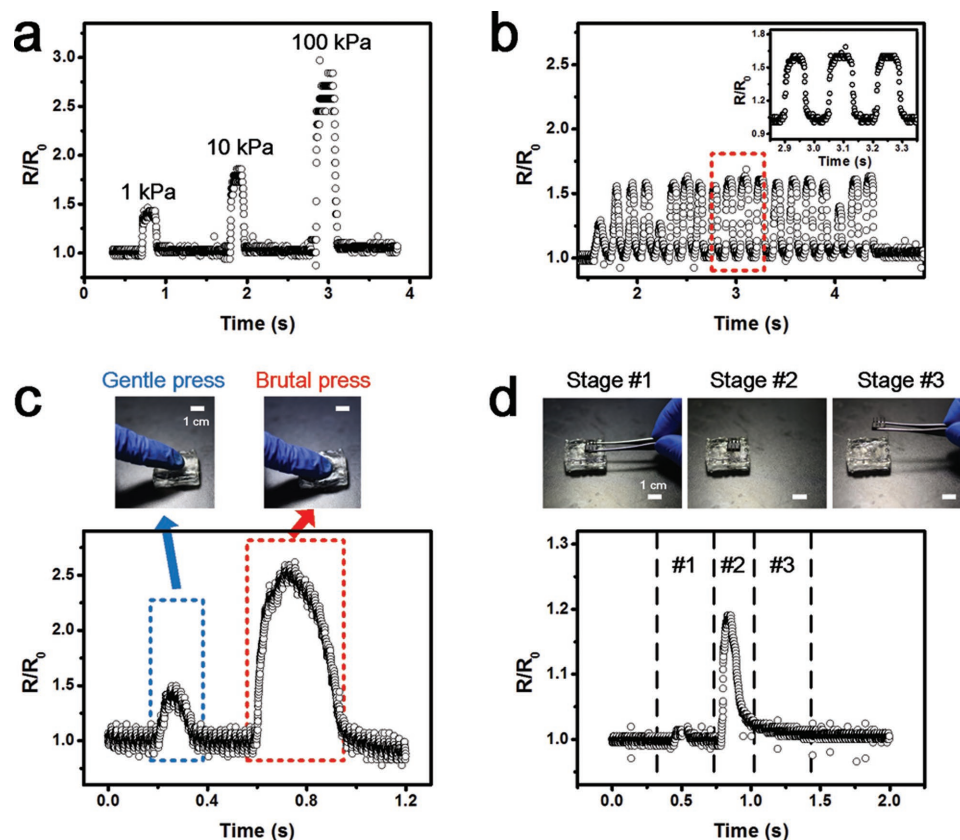


Figure 4. Application demonstration of a pressure sensor based on hydrogel electronics. a) Quantitative test result of the hydrogel pressure sensor with distinct responses to different levels of pressure (i.e., 1, 10, and 100 kPa). b) Cyclic performance of the hydrogel-based pressure sensor responding to a period of finger press (≈ 50 Hz). Inset: enlarged plot to show the response to cyclic press of a certain period indicated with a red-dotted square in the original plot. c) Response of the hydrogel-based pressure sensor to gentle and brutal finger presses, respectively. d) Response of the hydrogel-based pressure sensor to placing a tiny electronic component (an operational amplifier) on top of the hydrogel.

2.3. Application Demonstration of the Hydrogel Electronics as a Pressure Sensor

Based on the hydrogel electronics proposed in this work, a pressure sensor with vertically arranged helical layout of conductive liquid metal incorporated inside the hydrogel matrix is shown to prove its practical functionality (Figure 4; Movie S2, Supporting Information). The hydrogel pressure sensor presents excellent performance in distinguishing varying levels of pressure (i.e., 1, 10, and 100 kPa) (Figure 4a). Besides, experimental results show that the sensor responds steady to a period of rapid finger press (≈ 50 Hz) (Figure 4b). As a functional demonstration, it shows significantly different responses to gentle and brutal finger presses, respectively (Figure 4c). To depict the excellent sensitivity of the hydrogel-based pressure sensor, a small, light operational amplifier (length: 9 mm, width: 5 mm, mass: 0.45 g) was placed on top of the hydrogel and then removed, and corresponding waveform changes were recorded. As can be seen in Figure 4d, a distinct peak in the waveform comes out when the component touches the hydrogel sensor and further induces compression, and the waveform falls to the initial level when the amplifier is taken away. Such achievement of realizing hydrogel pressure sensor with sensitivity of 100 Pa and quick response paves its way for potential applications in

body-worn healthcare sensing systems for heartbeat, pulse, and blood pressure monitoring.

2.4. Application Demonstration of the Hydrogel Electronics as a Wearable Strain Sensor

To further testify the suitability of the reusable hydrogel electronics for cutting-edge wearable applications, an on-skin strain sensing device based on hydrogel electronics for human motion monitoring was demonstrated. In specific terms, a piece of hydrogel electronics was readily attached to the finger joint as a strain-sensing device (i.e., hydrogel sensor) (Figure 5a). And it can well differentiate motion of the finger with the help of an external-wired oscilloscope. The underlying monitoring mechanism is pretty simple that the hydrogel sensor remains unstretched when the finger is flat, while motion of the finger (e.g., bending) will induce stretch and corresponding resistance increase of the hydrogel sensor, resulting in obvious waveform changes displayed on the oscilloscope (Figure 5b). In addition, a double-finger motion monitoring system consisting of two pieces of hydrogel sensor is presented to simultaneously track the motion of both thumb and middle fingers (Figure 5c; Movie S3, Supporting Information). It is worthy of noting that in this

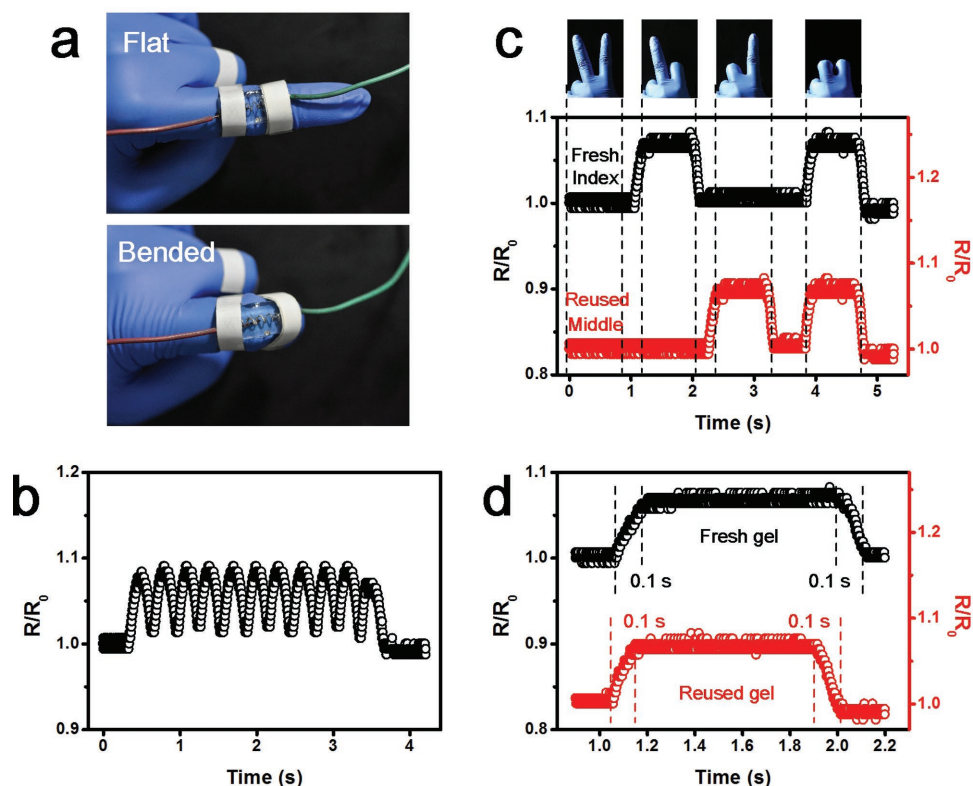


Figure 5. Application demonstration of a wearable strain sensing device based on hydrogel electronics for physical monitoring. a) Digital photos of the hydrogel strain sensor affixed to finger joint. b) Electrical response of the hydrogel strain sensor when finger is bended or stretched for multiple times. c) The dual sensing result from a fresh hydrogel sensor (index finger, black) and a reusable (after 12 drying–soaking cycles) hydrogel sensor (middle finger, red) reveals that the as-fabricated hydrogel electronics is able to simultaneously detect motions of multiple objects without cross-impact. And the reusable hydrogel electronics shows negligible inferiority in sensing function compared to the fresh hydrogel electronics. d) Quick response of the hydrogel sensor (≈ 0.1 s).

dual-monitoring system, the hydrogel sensor for middle finger motion monitoring has already endured twelve drying–soaking cycles before being affixed onto the finger joint. This reusable hydrogel sensor exhibits negligible difference in sensing function compared with the sensor fabricated with fresh hydrogel (index finger). The testing results also reveal that both the fresh and reusable hydrogel sensors in such system work independently with no cross-impact to each other and operate collaboratively to offer insight of the finger motion accurately and immediately (response time of ≈ 0.1 s) (Figure 5d). These satisfactory experimental outcomes further validate the great potential of the as-proposed hydrogel electronics for practical uses, including but not restricted to wearable healthcare devices and body-worn exoskeletons.

The novelty of our work here is that we combined soft and biocompatible hydrogels with tissue-like mechanical properties as substrate and ultraconductive liquid metal in 3D helical layout as conductive element to fabricate stretchable electronics with outstanding biofriendliness, mechanical stretchability, and functional robustness. These advantageous features are well catering to the demand for the most advanced wearable and implantable human healthcare applications, making hydrogel electronics promising for extensive applications in these rapidly developing areas. Moreover, the hydrogel-based stretchable electronics we developed enables reusing for multiple times as

validated by acceptable functionality resilience even after function failure because of hydrogel dehydration. This reusable capability is offering a promising solution to the recycling/disposal issue and practical difficulties in device collection/reprocessing of electronic products, especially considering the massive global electronic wastes made currently. Further, decreased number of electronics demanded result from reusing worn-out devices helps to save natural resources and raw materials required for electronics manufacturing. Additional economic concerns may well motivate consumers to prefer reusable electronics with relatively lower investment to their single-use counterparts. As far as we know, this is the very first study carried out to investigate reusable issues about stretchable electronics, which is helpful to propel these lab-made research outcomes to commercialized products in the nearest future.

Hydrogels are a family of polymeric materials with excellent biological compatibility as well as degradability. It seems that the degradation of hydrogel may hinder the long-term durability and some practical applications (e.g., long-time healthcare monitoring) of such hydrogel-based electronics. While in this work, the stretchable electronics based on PAA-alginate hydrogel shows superb durability of electrical conductivity even after being directly exposed to the air for up to five weeks (Figure S10, Supporting Information). More surprisingly, the hydrogel electronics can be stored in a vacuum

package with better sustained functionality (for ≈ 5 months) due to the isolation of moisture transfer between hydrogel and air (Figure S10, Supporting Information). And although the potential product from the degradation of PAA-alginate hydrogel (namely acrylamide) may induce cytotoxicity, PAA-alginate is generally regarded as a noncytotoxic hydrogel, and the in vivo negative effect on cell behavior as a result of hydrogel degradation can be well mitigated depending on the hydrogel concentration.^[31] On the other hand, employing hydrogels with various degrees of degradability may bring about possibility for fabricating electronics with controlled life cycle catering to different application purposes. For instance, some easily degradable natural hydrogels (e.g., collagen) can be suitable substrate candidates for biodegradable and transient electronics,^[32–34] which may facilitate implantable physiological monitoring of cardiac or cerebral functions, enabling a giant step toward precision medicine.

In this work, the thickness (≈ 5 mm) of the presented hydrogel electronics may be an inferior issue to weaken its sensitivity as skin-mountable or implantable sensors. The total thickness of the hydrogel electronics is determined by the commercially available helical springs (outer diameter of ≈ 2.5 mm), deployed to realize the 3D helical electronics layout with improved mechanical robustness and tolerance to large deformation compared with the conventional 2D serpentine conductive pattern. So there exists a trade-off for the hydrogel electronics between monitoring sensitivity and mechanical stability. Luckily, with the most advanced micro-/nanofabrication technique, it is promising to use miniaturized helical springs (even down to micro or nano scale) for the fabrication of thin-sheet hydrogel electronics with enhanced sensitivity and maintained robustness under stretch.

3. Conclusions

In conclusions, we have presented a facile microfluidic method to fabricate human-friendly, stretchable, and reusable electronics based on hydrogels, with commercially available, omnipresent helical springs. Due to the robust structure of 3D helical microfluidic channels inside hydrogel matrix and the fluid property of liquid metal (as conductive element filling the channel), the as-fabricated hydrogel electronics shows favorable electrical stability under cyclic mechanical stretch. Furthermore, based on the swelling capacity of hydrogel, we developed a scenario for reusing dehydrated and dysfunctional hydrogel electronics simply by hydration for the very first time. The hydrogel electronics dramatically falls in size and functionality when dehydrated. And a step of rehydration by simply casting into water can make its mechanical and electrical functionality recovered. The final demonstrations of a sensitive pressure sensor and an on-skin dual strain-sensing device further uncover the promising perspective of hydrogel electronics for the cutting-edge, human-friendly wearable applications.

4. Experimental Section

Fabrication of the Hydrogel Electronics: Laser-etched (Universal VLS 2.30, USA) poly(methyl methacrylate) (PMMA) boards with bolts were mechanically assembled into a casting mold (inner dimension: length:

24 mm, width: 12 mm, height: 5 mm), and a stainless helical spring (wire diameter: 300 μm , outer diameter: 2.5 mm, pitch gauge: 2 mm) was inserted into the mold through a hole on the sidewall of it. Then the precursor solution of hydrogel was poured into the PMMA mold. After the gelation of hydrogel, the helical spring was rotated out of the mold, resulting in a transparent 3D helical microchannel inside the hydrogel matrix. Subsequently, liquid metal (Eutectic Gallium Indium, Sigma Aldrich, USA) was injected into the channel and copper wires were connected to both ends of the channel to facilitate interconnection of the hydrogel electronics with outer circuits. Next, sealing on both sides of the hydrogel (microchannel) finalized the microfluidic fabrication process of hydrogel electronics.

In this work, polyacrylamide (PAA)-alginate was employed as a demonstration model for microfluidic fabrication of hydrogel electronics. The synthesis of PAA-alginate hydrogel started with dissolving acrylamide (AA, 12.45 wt%) and alginate (1.55 wt%) powders in deionized water. Crosslinker *N,N'*-methylenebisacrylamide (MBA, 0.0085 wt%) and thermal initiator ammonium persulfate (AP, 0.025 wt%) were then added to the solution. After degassing in the vacuum chamber at room temperature for 15 min, accelerator *N,N,N',N'*-tetramethylethylenediamine (TEMED, 0.0775 wt%) was added to obtain PAA-alginate precursor solution. Next, the precursor was poured into the PMMA mold. The PMMA mold filled with PAA-alginate precursor was then successively transferred into an oven at 70 °C for 3 h and immersed into 0.1 M CaCl_2 solution for another 3 h to finally produce PAA-alginate hydrogel. The sealing of hydrogel electronics in this demonstration was realized by crosslinking a thin layer of PAA gel.

Finite Element Simulation of the Hydrogel Electronics: To identify the stress/strain field of hydrogel electronics under different strain loadings, a series of numerical simulations were performed using commercially available software (COMSOL Multiphysics 5.0, COMSOL, Sweden). Due to the slow diffusion of solvent molecules compared with the stretch process, the hydrogel matrix was treated as isotropic solid material with Young's modulus of 10 kPa. The liquid metal was simplified as incompressible material with much smaller Young's modulus of 10 Pa. The Poisson ratio of hydrogel matrix is 0.45 and that of liquid metal was fixed as 0.49 due to its incompressibility. All displacements were constrained to be zero on the right side of hydrogel electronics sample. The other side of sample was given a prescribed displacement of 12 mm (50% strain), 24 mm (100% strain), and 36 mm (150% strain), as what were done in experiments. And simulations were further performed under 200% strain (48 mm), 250% strain (60 mm), and 300% strain (72 mm) to predict the mechanical field of hydrogel electronics under larger deformation.

Tensile Test of the Hydrogel Electronics: The tensile test of the hydrogel electronics was implemented with a tensile instrument (ElectroForce 3200 Series III, Bose, USA). The testing samples were fabricated into a dumbbell shape (length: 24 mm, width: 10 mm, thickness: 3 mm, gauge length: 4 mm, gauge width: 4 mm) through the help of PMMA molds. After being affixed to the clamps, the sample was stretched at a constant velocity of 10 mm min^{-1} by the tensile instrument. The stress–strain curve was recorded during the tensile test process, and the Young's modulus was then calculated by the average slope over 0%–10% strain ration of the curve.

Wearable Function Demonstration of the Hydrogel Electronics: The wearable function demonstration circuit was built through wire connecting hydrogel electronics with a DC power supply and some hard resistors integrated on a bread board. The change of voltage amplitude as a result of finger bending/stretching was displayed on an oscilloscope (UTD2102CM, UNI-T, China). All the demonstrations of finger gestures (e.g., pressing and bending) were conducted by the leading author with informed consent.

Supporting Information

Supporting Information is available from the Wiley Online Library or from the author.

Acknowledgements

This work was financially supported by the National Natural Science Foundation of China (21775117, 11522219, 11532009), the International Science and Technology Cooperation and Exchange Program of Shaanxi Province of China (2016KW-064), and the General Financial Grant from the China Postdoctoral Science Foundation (2016M5927736).

Conflict of Interest

The authors declare no conflict of interest.

Keywords

function resilience, hydrogels, reusability, stretchable electronics, wearable force sensors

Received: May 4, 2018

Revised: June 12, 2018

Published online: July 30, 2018

-
- [1] S. K. Kang, R. K. Murphy, S. W. Hwang, S. M. Lee, D. V. Harburg, N. A. Krueger, J. Shin, P. Gamble, H. Cheng, S. Yu, Z. Liu, J. G. McCall, M. Stephen, H. Ying, J. Kim, G. Park, R. C. Webb, C. H. Lee, S. Chung, D. S. Wie, A. D. Gujar, B. Vemulapalli, A. H. Kim, K. M. Lee, J. Cheng, Y. Huang, S. H. Lee, P. V. Braun, W. Z. Ray, J. A. Rogers, *Nature* **2016**, *530*, 71.
- [2] J. Liu, T.-M. Fu, Z. Cheng, G. Hong, T. Zhou, L. Jin, M. Duvvuri, Z. Jiang, P. Kruskal, C. Xie, Z. Suo, Y. Fang, C. M. Lieber, *Nat. Nanotechnol.* **2015**, *10*, 629.
- [3] S.-W. Hwang, H. Tao, D.-H. Kim, H. Cheng, J.-K. Song, E. Rill, M. A. Brenckle, B. Panilaitis, S. M. Won, Y.-S. Kim, Y. M. Song, K. J. Yu, A. Ameen, R. Li, Y. Su, M. Yang, D. L. Kaplan, M. R. Zakin, M. J. Slepian, Y. Huang, F. G. Omenetto, J. A. Rogers, *Science* **2012**, *337*, 1640.
- [4] S. Choi, H. Lee, R. Ghaffari, T. Hyeon, D. H. Kim, *Adv. Mater.* **2016**, *28*, 4203.
- [5] D.-H. Kim, N. Lu, R. Ma, Y.-S. Kim, R.-H. Kim, S. Wang, J. Wu, S. M. Won, H. Tao, A. Islam, K. J. Yu, T.-i. Kim, R. Chowdhury, M. Ying, L. Xu, M. Li, H.-J. Chung, H. Keum, M. McCormick, P. Liu, Y.-W. Zhang, F. G. Omenetto, Y. Huang, T. Coleman, J. A. Rogers, *Science* **2011**, *333*, 838.
- [6] D. Son, J. Lee, S. Qiao, R. Ghaffari, J. Kim, J. E. Lee, C. Song, S. J. Kim, D. J. Lee, S. W. Jun, S. Yang, M. Park, J. Shin, K. Do, M. Lee, K. Kang, C. S. Hwang, N. Lu, T. Hyeon, D.-H. Kim, *Nat. Nanotechnol.* **2014**, *9*, 397.
- [7] T. Yamada, Y. Hayamizu, Y. Yamamoto, Y. Yomogida, A. Izadi-Najafabadi, D. N. Futaba, K. Hata, *Nat. Nanotechnol.* **2011**, *6*, 296.
- [8] T. Q. Trung, N. E. Lee, *Adv. Mater.* **2016**, *28*, 4338.
- [9] R. Zhong, Q. Tang, S. Wang, H. Zhang, F. Zhang, M. Xiao, T. Man, X. Qu, L. Li, W. Zhang, H. Pei, *Adv. Mater.* **2018**, *30*, 1706887.
- [10] H. Lee, C. Song, Y. S. Hong, M. S. Kim, H. R. Cho, T. Kang, K. Shin, S. H. Choi, T. Hyeon, D.-H. Kim, *Sci. Adv.* **2017**, *3*, e1601314.
- [11] M. Nassar Joanna, D. Cordero Marlon, T. Kutbee Arwa, A. Karimi Muhammad, A. T. Sevilla Galo, M. Hussain Aftab, A. Shamim, M. Hussain Muhammad, *Adv. Mater. Technol.* **2016**, *1*, 1600004.
- [12] F. Xu, T. D. Finley, M. Turkyaydin, Y. R. Sung, U. A. Gurkan, A. S. Yavuz, R. O. Guldiken, U. Demirci, *Biomaterials* **2011**, *32*, 7847.
- [13] F. Xu, C. A. M. Wu, V. Rengarajan, T. D. Finley, H. O. Keles, Y. R. Sung, B. Q. Li, U. A. Gurkan, U. Demirci, *Adv. Mater.* **2011**, *23*, 4254.
- [14] J. B. Leach, C. E. Schmidt, *Biomaterials* **2005**, *26*, 125.
- [15] M. Cully, *Nat. Rev. Drug Discovery* **2015**, *14*, 678.
- [16] G. W. Ashley, J. Henise, R. Reid, D. V. Santi, *Proc. Natl. Acad. Sci. USA* **2013**, *110*, 2318.
- [17] M. Sasaki, B. C. Karikkineth, K. Nagamine, H. Kaji, K. Torimitsu, M. Nishizawa, *Adv. Healthcare Mater.* **2014**, *3*, 1919.
- [18] T. Lu, L. Finkenauer, J. Wissman, C. Majidi, *Adv. Funct. Mater.* **2014**, *24*, 3351.
- [19] N. Matsuhisa, M. Kaltenbrunner, T. Yokota, H. Jinno, K. Kuribara, T. Sekitani, T. Someya, *Nat. Commun.* **2015**, *6*, 7461.
- [20] J. Y. Sun, C. Keplinger, G. M. Whitesides, Z. Suo, *Adv. Mater.* **2014**, *26*, 7608.
- [21] H. Yuk, T. Zhang, G. A. Parada, X. Liu, X. Zhao, *Nat. Commun.* **2016**, *7*, 12028.
- [22] S. Lin, H. Yuk, T. Zhang, G. A. Parada, H. Koo, C. Yu, X. Zhao, *Adv. Mater.* **2016**, *28*, 4497.
- [23] Y. Wang, S. Gong, S. J. Wang, G. P. Simon, W. Cheng, *Mater. Horiz.* **2016**, *3*, 208.
- [24] A. Bin Imran, K. Esaki, H. Gotoh, T. Seki, K. Ito, Y. Sakai, Y. Takeoka, *Nat. Commun.* **2014**, *5*, 5124.
- [25] X. Chen, H.-H. Dai, *Acta Mech. Sin.* **2015**, *31*, 627.
- [26] M. D. Dickey, R. C. Chiechi, R. J. Larsen, E. A. Weiss, D. A. Weitz, G. M. Whitesides, *Adv. Funct. Mater.* **2008**, *18*, 1097.
- [27] Y. Long Han, H. Liu, C. Ouyang, T. Jian Lu, F. Xu, *Sci. Rep.* **2015**, *5*, 11488.
- [28] K. I. Jang, K. Li, H. U. Chung, S. Xu, H. N. Jung, Y. Yang, J. W. Kwak, H. H. Jung, J. Song, C. Yang, A. Wang, Z. Liu, J. Y. Lee, B. H. Kim, J. H. Kim, J. Lee, Y. Yu, B. J. Kim, H. Jang, K. J. Yu, J. Kim, J. W. Lee, J. W. Jeong, Y. M. Song, Y. Huang, Y. Zhang, J. A. Rogers, *Nat. Commun.* **2017**, *8*, 15894.
- [29] F. Xu, T. Lu, *Introduction to Skin Biothermomechanics and Thermal Pain*, Vol. 7, Springer, Berlin **2011**.
- [30] D. Wirthl, R. Pichler, M. Drack, G. Kettlguber, R. Moser, R. Gerstmayr, F. Hartmann, E. Bradt, R. Kaltseis, C. M. Siket, S. E. Schausberger, S. Hild, S. Bauer, M. Kaltenbrunner, *Sci. Adv.* **2017**, *3*, e1700053.
- [31] M. C. Darnell, J. Y. Sun, M. Mehta, C. Johnson, P. R. Arany, Z. Suo, D. J. Mooney, *Biomaterials* **2013**, *34*, 8042.
- [32] S. W. Hwang, J. K. Song, X. Huang, H. Cheng, S. K. Kang, B. H. Kim, J. H. Kim, S. Yu, Y. Huang, J. A. Rogers, *Adv. Mater.* **2014**, *26*, 3905.
- [33] S.-W. Hwang, C. H. Lee, H. Cheng, J.-W. Jeong, S.-K. Kang, J.-H. Kim, J. Shin, J. Yang, Z. Liu, G. A. Ameer, Y. Huang, J. A. Rogers, *Nano Lett.* **2015**, *15*, 2801.
- [34] K. J. Yu, D. Kuzum, S.-W. Hwang, B. H. Kim, H. Juul, N. H. Kim, S. M. Won, K. Chiang, M. Trumpis, A. G. Richardson, H. Cheng, H. Fang, M. Thompson, H. Bink, D. Talos, K. J. Seo, H. N. Lee, S.-K. Kang, J.-H. Kim, J. Y. Lee, Y. Huang, F. E. Jensen, M. A. Dichter, T. H. Lucas, J. Vivoti, B. Litt, J. A. Rogers, *Nat. Mater.* **2016**, *15*, 782.